MATERIALE PLASTICE
https://revmaterialeplastice.ro
https://doi.org/10.37358/Mat.Plast.1964

Optimal Deformation of a Small Plastic Light-guide Using Machine Learning Algorithms

MIN JI YOO[1], SEONG YEOL HAN[2*]
[1]Kongju National University, Department of Optical Engineering & Metal Mold, 1223-24, Cheonan-daero, Seobuk-gu, Cheonan-si, Chungcheongnam-do, Republic of Korea
[2]Kongju National University, Department of Metalmold Design Engineering, 1223-24, Cheonan-daero, Seobuk-gu, Cheonan si, Chungcheongnam-do, Republic of Korea

Abstract: *Lensknob is a component that transmits light to users. It is essential to minimize the deformation to transmit the light uniformly. As a method of finding injection molding parameters capable of minimizing the deformation, the amount of deformation of the Lensknob was predicted in advance by numerical analysis of the injection molding. However, because it takes a considerable amount of time to analyze, we used the Decision tree as a Machine Learning model. As the injection molding parameters, we set the melting temperature, cooling time, holding time, holding pressure, and ram speed. We set the injection molding parameters based on the range recommended by Moldflow. A full factor method of factor 5 level 3 was applied in the experiment. We predicted the parameters for minimizing the deformation through the Decision tree learned with 243 experimental data. We set the criteria to evaluate the performance of the Decision tree. The parameters predicted by the Decision tree improved the deformation by about 10.37%.*

Keywords: *injection molding, CAE, Decision tree, process parameters, deformation, optimization*

1.Introduction

Light-guide injection products are parts that uniformly diffuse light from light sources and transmit a constant luminance to users. Light-guide parts are also assembled in knobs located in the center fascia of automobiles (a control panel space where various buttons for manipulating functions such as audio and air conditioner are gathered). In this study, light-guide components assembled to these knobs were used. The part is called a Lensknob. Figures 1a and 1b show the modeling of the automobile center fascia and Lensknob, respectively. The Lensknob is manufactured using transparent polycarbonate (PC) resin characterized by high dimensional accuracy and luminance uniformity. Injection-molded parts requiring optical properties require more precise process parameters than general injection molded parts [1-5].

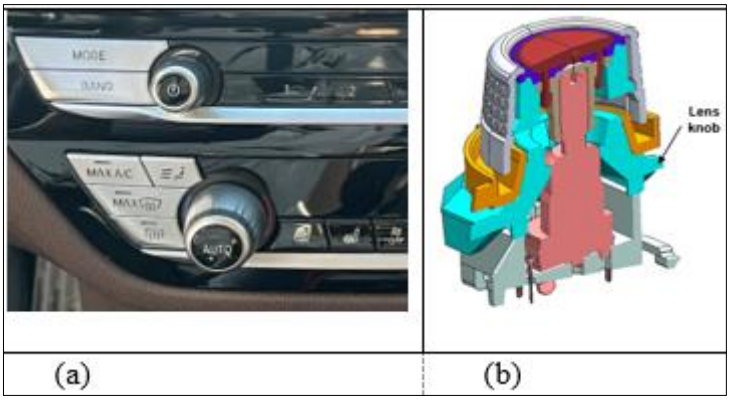

Figure 1. a) Center fascia of automobiles b) Lensknob assemble

**email: srhan@kongju.ac.kr*

Injection molding simulation is used to control molding parameters for precise injection molding. Injection molding simulation can predict the overall flow, cooling, and deformation processes for injection molding processes and predict potential problems such as sink marks, air traps, and short shots [6-10]. However, when simulating a small, molded article that requires sophisticated dimensional precision, there is a disadvantage in that the time needed for the analysis increases due to the increase in the number of meshes.

For this reason, we can use machine learning algorithms to control faster and more sophisticated molding parameters. Machine learning algorithms are a subset of artificial intelligence that computers use to analyze, learn, and make decisions based on what they have learned. Recently, more studies have been published that make predictions using machine learning algorithms for injection molding.

As a related study on the optimization of injection molding, Gao et al. proposed an optimization method using a Kriging surrogate model to minimize the warpage of the injection molding in the study. By introducing an adaptive optimization method using the Kriging surrogate model, they reduced the warpage of a mobile phone-shaped molded product by 38%. Additionally, they reduced the deformation of the box model molded products by 24.6% in the same manner [11-12]. Gao et al. investigated the relationship between the shear viscosity and the pressure-specific volume–temperature (pvT) of low-density polyethylene (LDPE). The investigation of the pvT relationship shows that the total warpage increases when the pvT model constant is adjusted to mimic fast cooling parameters [13]. Hwang et al. predicted process parameters capable of minimizing deformation using a decision-tree. The predicted model showed a confidence level of 97.5%, and there was an improvement effect of 7.7% compared to the existing deformation [14]. Ahmed et al. conducted a study to develop a prediction model to optimize the deformation of PVC injection molded products as drip chambers of medical syringes using ensemble machine learning algorithms. They developed a predictive model by applying the Random forest model and the Gradient Boosted regression tree. The Random forest model showed a 96.75% accuracy, and the Gradient Boosted regression tree showed an accuracy of 90.63% [15]. Chen et al. used the Taguchi method, adding backpropagation neural networks genetic algorithms to optimize the injection molding. To summarize, they confirmed that the proposed system effectively optimizes the setup procedures of multiple-input single-output (MISO) plastic injection molding and can significantly benefit quality and cost [16]. Many studies have optimized the process of injection molding using an artificial neural network (ANN). Yang et al. confirmed a high level of accuracy and reliability with an average deviation from the target mass of 0.15+0.07 g using an ANN [17]. Moayyedian et al. applied Taguchi methods to demonstrate compatibility between the ANN model and the Taguchi method at 1.5 percent [18]. Altan et al. investigated the effect of injection molding of samples of the same shape on each contraction using PP and PS. They confirmed an excellent error accuracy of 8.6% (PP) and 0.48% (PS) [19]. Tercan et al. using Transfer-learning based on the ANN, confirmed that Transfer-learning accelerates the network learning phase and improves the predictive performance with fewer data values [20]. Ke et al. propose a multi-layer perceptron (MLP) neural network model combined with quality indicators to quickly and automatically predict the geometry of the finished product. The results indicate that the training and testing of the one-stage holding pressure index, pressure integration index, residual pressure drop index, and peak pressure index for geometric width are accurate (accuracy exceeds 92%), demonstrating the proposed method's feasibility [21]. Lee et al. conducted a study to derive the optimal injection parameters for mold products using a deep neural network (DNN) algorithm that added a hidden layer to the ANN. The predicted value obtained an accuracy of 0.8–0.9. However, they could not confirm more accurate expectations due to the limitation of the amount of data. [22]. Shi et al. proposed the ANN model and expected improvement (EI) function integration scheme, and they confirmed that this method could efficiently reduce deformation and converge quickly to optimized solutions [23]. Ozcelik et al. proposed an effective optimization method using the ANN and genetic algorithms. In conclusion, genetic algorithm (GA) reduced the deformation of the initial model signal and improved the deformation by 51% [24]. Kurtaran et al. confirmed that the

deformation of a bus ceiling lamp base was reduced by 46.5% using the ANN and GA [25]. Tsai et al. combined the ANN and GA to create an inverse model to improve the accuracy of an optical lens shape. The results obtained using the inverse model met the accuracy of the optical lens form [26]. Shen et al. propose a method that combines artificial neural networks and genetic algorithms (ANN/GA) to optimize the injection molding process. In this method, they develop a BP neural network model to map complex nonlinear relationships between process conditions and quality indices of injection molded parts and use GA for process condition optimization as a fitness function based on the ANN model. The results show that the combined ANN/GA method effectively optimizes the injection molding process [27]. Xu et al. proposed an artificial neural network and particle cluster optimization (PSO) algorithm combination method, which reduced the maximum von Mises stress of the initial model by 12.9% [28].

This study used Decision tree and computer- aided engineering (CAE) to derive molding process parameters capable of minimizing the deformation of Lensknob molded products. The surrogate model uses Moldflow software. Moldflow estimates the injection molded product's quality by predicting the polymer's flow according to the process condition setting. In Moldflow, polymer flow is non-Newtonian, non-isothermal, and incompressible behavior and the governing equation uses mass conservation, momentum conservation, and energy conservation equations as the basis. Injection molding analysis can predict the quality of the molded product without actually performing injection molding. However, it takes a considerable amount of computing consumed time to simulate many cases. We can reduce this consumed time by using the decision tree. Unlike machine learning models ANN and DNN used to predict the quality of injection molding, Decision Tree has the advantage of transparently checking the process in which the predicted value is determined. The results of this paper show that the method using a Decision tree and injection molding analysis contributed to deformation-optimization.

The remainder of this paper consists of: Section 2 provides detailed information and methodology on injection molding analysis. Section 3 implements deformation optimization by applying a decision tree and evaluating the values predicted by the decision tree.

2. Materials and methods

2.1. Injection molding analysis of the Lensknob

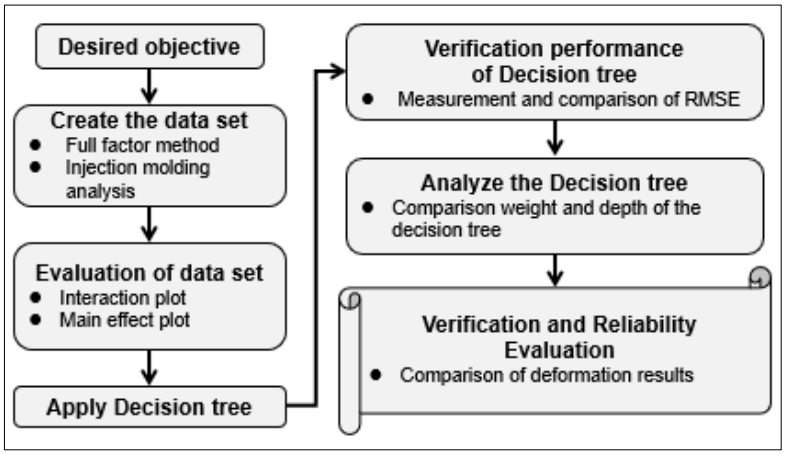

Figure 2. Flowchart of research progress

Figure 2 shows the flowchart that describes the progress of this study. Figure 3 shows the Lensknob used in this study. The center of the Lensknob is circular, and there are several ribs on the back. It consists of three products of different sizes. Figure 3a is the front surface of the molded product, and each product is indicated by ①, ②, and ③. The size of the molded part is about ① 29*24*16 mm, ② 32*26*18 mm, ③ 31*28*20 mm, and the average thickness is about 2 mm.

Samyang Company's PC Trirex 3022IR was used as the resin for the injection molding analysis. Figure 4 shows the pressure-specific volume–temperature (pvT) diagram of the PC Trirex 3022IR. In addition, Table 1 shows the range of the mold temperature and melt temperature parameters of the PC Trirex 3022IR recommended by Moldflow

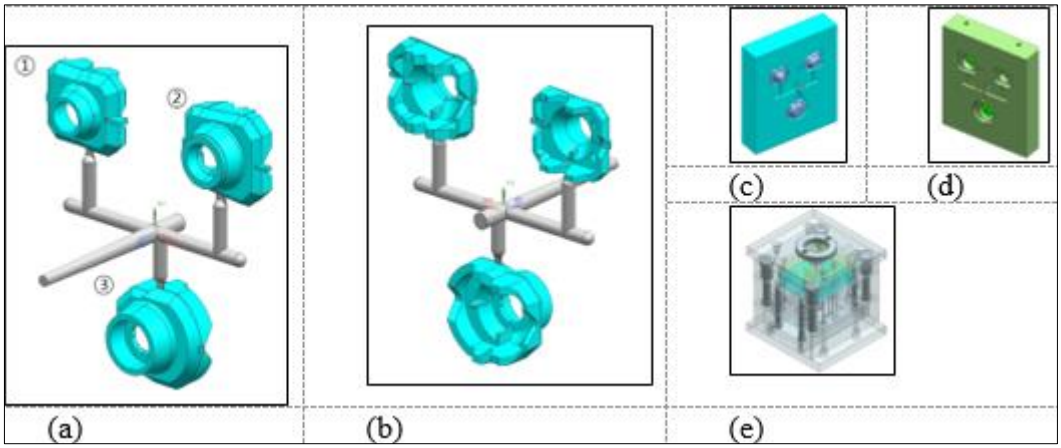

Figure 3. 3D model: a) front side b) back side c) moving core plate d) fixed core plate e) full of mold

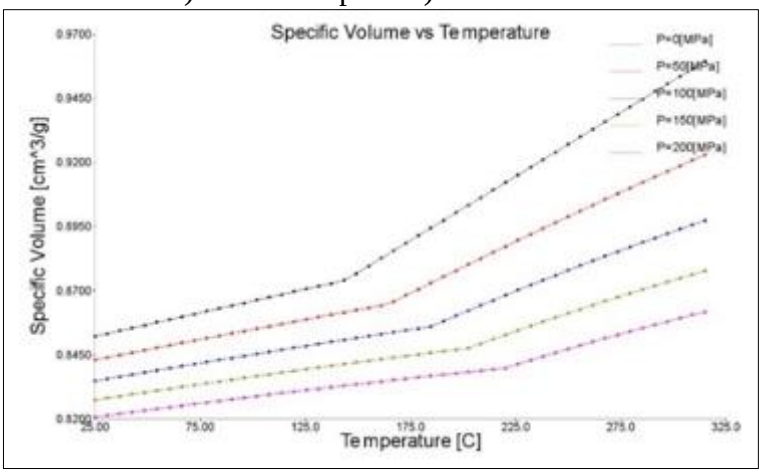

Figure 4. The pvT properties of the PC Trirex 3022IR

Table 1. Recommended range of the injection molding process parameter (unit: *°C*)

PC Trirex 3022IR	Mold temperature	Melt temperature
Lower limit	70	275
Upper limit	90	315

Figure 5. Experiment injection molding machine (IDE100EN II)

Figure 5 shows the injection molding machine, and Figure 6 shows the actual injection mold applied to this study. Figure 6b and c show the moving plate and the fixed plate of the mold. The size of the mold is 200 (horizontal)×230 (vertical)×250 (height) (mm), which uses a cold gate. The injection molding machine is the IDE100EN II from the LG company with a maximum molding force of 100 tons, a maximum injection amount of 150 g, and a maximum injection pressure of 170 MPa. Figure 6a and b show the actual injection-molded Lensknob and the front and back of the Lensknob, respectively.

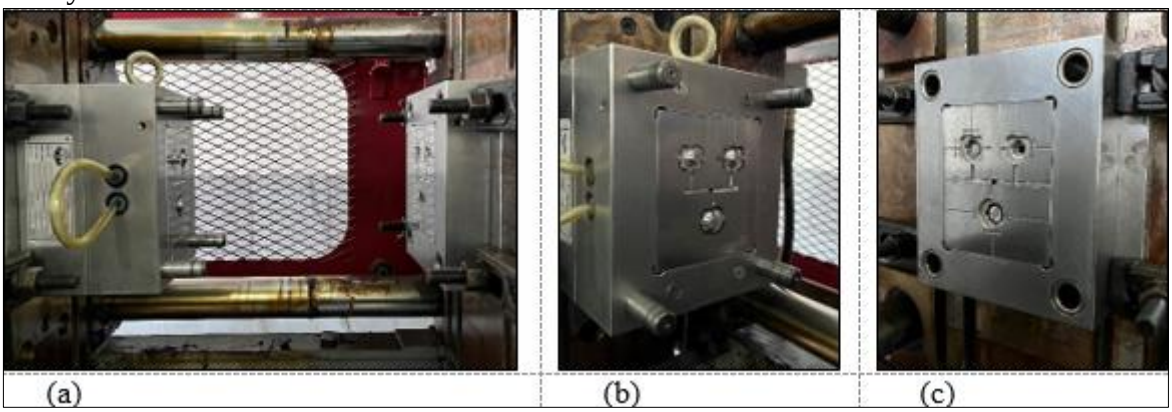

Figure 6. Lensknob mold: a) installed mold b) moving half c) fixed half

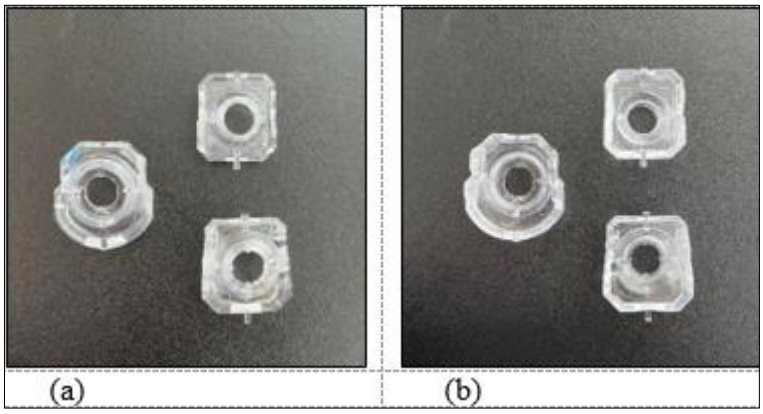

Figure 7. Molded lensknob: a) front b) back

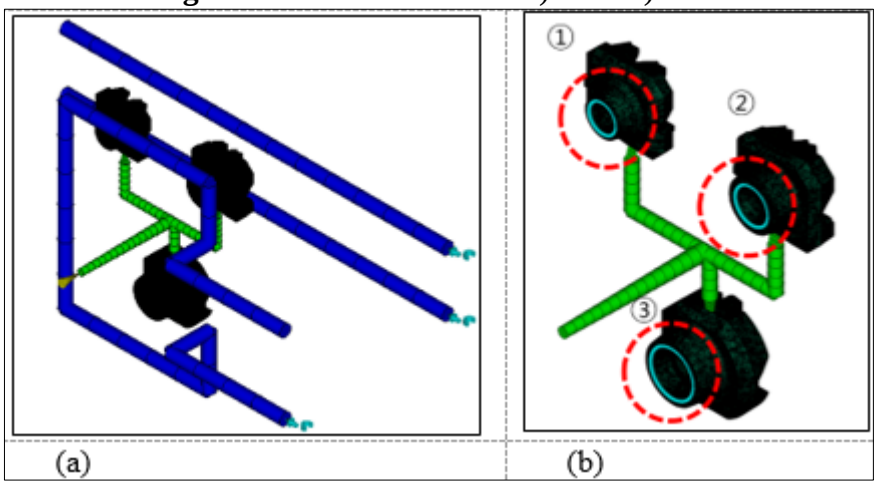

Figure 8. Analysis model: a) feed system and cooling channel b) measurement nodes

We used Moldflow 2021 from Autodesk for the injection molding analysis program. The type of mesh used was 3D tetra with 2.93 million meshes. Figure 7a shows the analysis model of the

Lensknob, and Figure 7b shows the position of the nodes selected to measure the concentricity of each part. The Lensknob is a transparent product. Because light must be uniformly transmitted due to the nature of the Lensknob molded product, uniformity of the circular shape at the center of the Lensknob is essential. Therefore, we measured the concentricity of the circular portion located in the center of the Lensknob. We used the roundness among the command line functions on Moldflow when measuring concentricity shown in Figure 8.

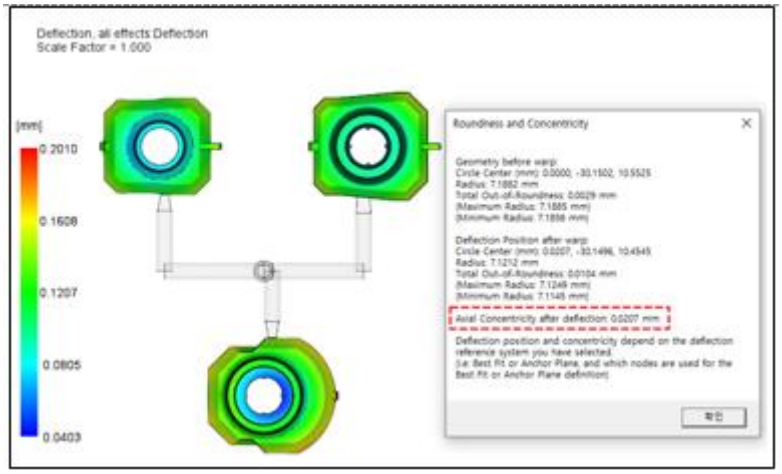

Figure 9. Axial concentricity after deformation

2.2. Creating the data set

Table 2. Factors and levels

	Factor	Unit	Level		
A	Melt temperature	˚C	275	295	315
B	Cooling time	s	12	16	20
C	Holding time	s	1.4	2.7	4
D	Holding pressure	MPa	60	66	72
E	Ram speed	mm/s	10	15	20

In this study, the melt temperature, cooling time, holding time, holding pressure, and ram speed were selected as factors considered to affect the deformation of the Lensknob. These factors were based on the recommended range in Moldflow. The details are presented in Table 2. They were composed of 5 factors and three levels, and a total of 243 injection molding analyses was performed by applying the full factorial method. Table 3 shows 243 process parameters and the results of the axial concentricity after deformation for each molded product accordingly. We referred to the axial concentricity after deflecting each molded part ①, ②, and ③ as D_1, D_2, and D_3, and their average was set as D_{avg}. Table 4 shows the fill time, maximum injection pressure, clamp force, and mold temperature predicted by Moldflow in the 243 injection molding analyses. The optimization problem of the axial concentricity after deformation can be written as Equation (1).

$$\begin{aligned} &Find: X_n \;\; n = A, B, C, D, E \\ &\quad min: D_{avg} \\ &\quad subject\ to: 275 \le X_A \le 315 \\ &\qquad\qquad\quad 12 \le X_B \le 20 \\ &\qquad\qquad\quad 1.4 \le X_C \le 20 \\ &\qquad\qquad\quad 60 \le X_D \le 72 \\ &\qquad\qquad\quad 10 \le X_E \le 20 \\ &\quad and\ D_1 \le 0.0042;\ D_2 \le 0.0058;\ D_3 \le 0.0207 \end{aligned} \tag{1}$$

Table 3. Detail on the 243 experiments

No.	A	B	C	D	E	D_1	D_2	D_3	D_{avg}
1	295	12	4	66	15	0.0041	0.0056	0.0207	0.0101
2	275	20	2.7	60	10	0.0040	0.0055	0.0204	0.0100
3	295	20	1.4	66	15	0.0042	0.0066	0.0208	0.0105
⋮									
241	295	12	1.4	66	15	0.0041	0.0064	0.0207	0.0104
242	275	16	4	60	15	0.0040	0.0054	0.0205	0.0100
243	275	20	1.4	72	20	0.0038	0.0062	0.0199	0.0100
Avg	-					0.0042	0.0058	0.0207	0.0102

Table 4. Results of the 243 injection molding analyses

No.	Fill time	Maximum injection pressure	Clamp force	Mold temp.
1	0.7531	75.65	13.58	88.84
2	0.7533	90.94	11.68	81.09
3	0.7522	74.15	13.61	82.90
⋮				
241	0.7531	75.65	13.60	88.84
242	0.7544	89.61	11.51	83.55
243	0.5646	92.68	14.54	81.09
Avg	0.8149	77.16	13.49	85.41

3. Results and discussions

3.1. Analysis of the data set

We analyzed the interaction and main effects to determine the correlation between the five process parameters and target before analyzing the resulting data to train the Decision tree. Figures 10a and 10b are diagrams showing the interaction and main effect of the factors on the average concentricity bias. The interaction plot interprets that interaction does not occur when the lines are parallel. In other words, there is no interaction. Therefore, we can interpret the main effect without considering the interaction effect. The main effect diagram interprets that an effect exists when the line is not horizontal. The main effect is more significant as the slope of the graph line is steep. Therefore, it is confirmed that the main effect of the melt temperature is the greatest, and the main effect of the cooling time is the smallest.

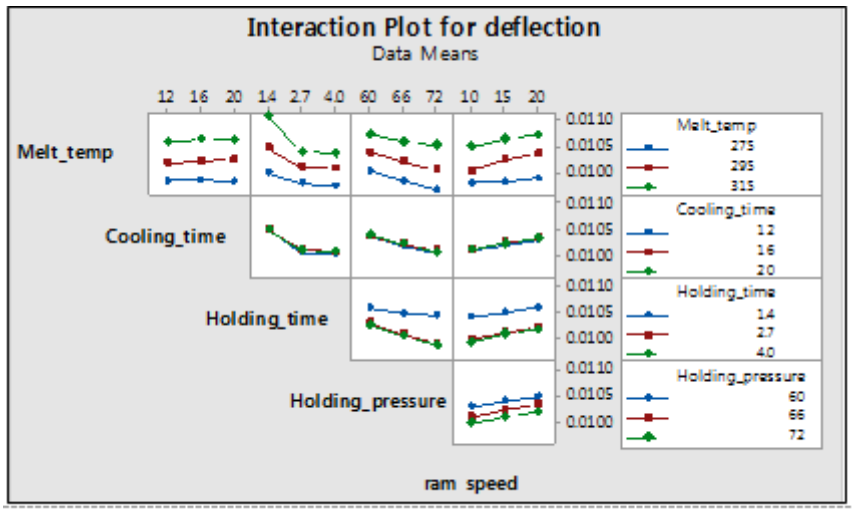

(a)

(b)

Figure 10. a) Interaction Plot for the average of the Deformation b) Main effects plot for the average of the deformation

3.2. Decision tree

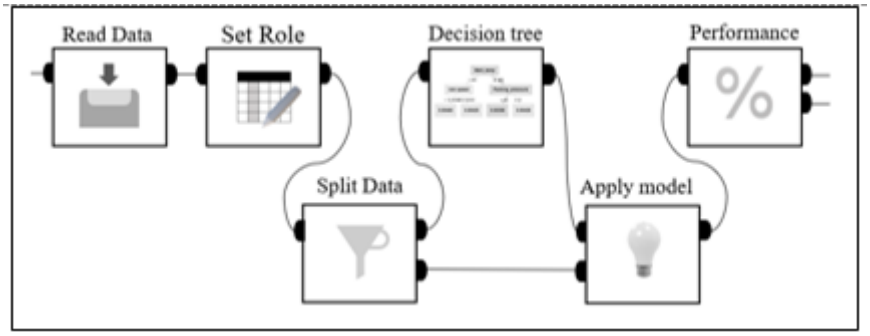

Figure 11. Process of applying the Decision tree

We used RapidMiner Studio Version Educational 9.10 to create a Decision tree model. The advantage of the Decision tree is that due to its high explanatory power, it is easy to grasp which variables influence the predicted value and are relatively less sensitive to outliers than other machine learning models [29]. Figure 11 briefly describes the process from data input to performance evaluation. First, 243 analysis results are inputted as training data. The 'Set Role' operator designates the average concentricity measurements as a target. 'Split Data' operator distributes the data at 80% training and 20% testing. The 'Apply Model' operator evaluates the test data using the 'Decision tree' learned with the training data, and the 'Performance' operator evaluates the statistical performance of the model.

Before analyzing the prediction of the Decision tree, we compared the predictive performance with the Generated Linear Model, Deep Learning, and Support Vector Machine models to verify the signature of the Decision tree. Figure 12 and Table 5 show the root mean square error (RMSE) of the Decision tree, Deep learning, Generalized linear model, and Support vector machine model. RMSE is based on equation (2).

$$\text{RMSE} = \sqrt{\frac{1}{n}\sum_{i=1}^{n}(y_i - \hat{y}_i)^2} \qquad (2)$$

y_i: true values
$\hat{y}_i$: predicted values

RMSE is one of the most commonly used indicators for evaluating regression analysis, and it is interpreted that as the value gets closer to 0, the performance gets better. All four models manifested good reliability within 0.00043, and the RMSE of the Decision tree model was the lowest at 0.00015, so we verified that it displayed the best performance among the comparative models.

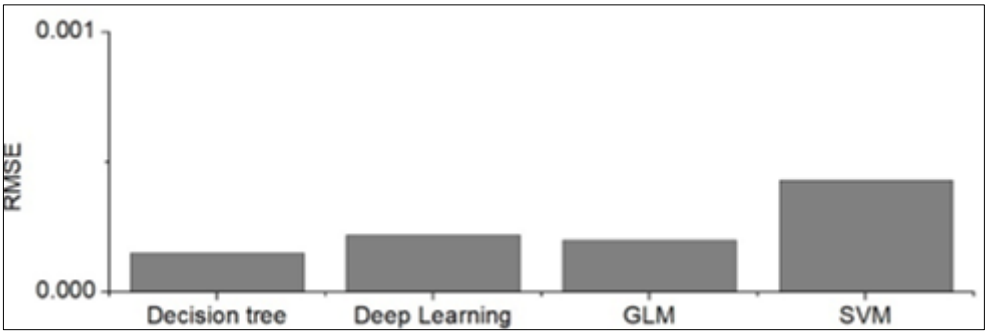

Figure 12. RMSE value compared to the other models

Table 5. RMSE value compared to the other models

Model	RMSE
Decision tree	0.00015
Deep learning	0.00022
Generalized linear model	0.00020
Support vector machine	0.00043

3.3. Analysis of the Decision tree

The Decision tree is like a collection of nodes for generating a target predictive optimal value. Each node divides for one specific attribute and repeats the creation of a new node until the criteria are met. In the case of a regression model in the Decision tree, the estimate is expressed as a number. And the attribute weight represents the functional importance of a given attribute. It is the sum of the attributes selected when splitting while improving according to the criteria chosen by the node [30]. Figure 13 is a graph showing the weights according to the attributes. The melt temperature had the highest weight, followed by the ram speed, holding pressure, holding time, and cooling time. We can predict that the melting temperature is the most relevant variable when generating the predicted value. In addition, we can expect that the cooling time has the most negligible impact when generating the predicted value.

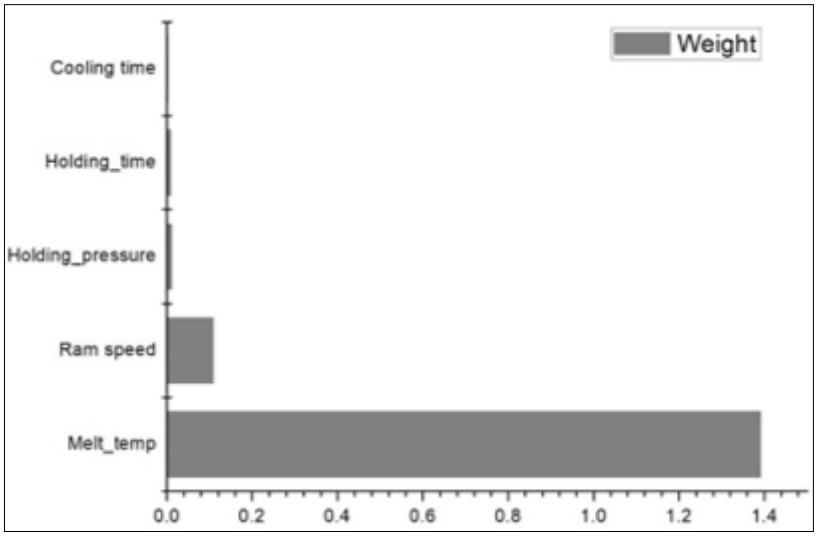

Figure 13. Weight according to the parameters

Figure 14a shows a brief concept of the depth of the Decision tree. Figure 14b represents the error rate according to the Maximal Depth of the Decision tree. The maximum depth means the most profound depth between the divided Leaf node and Root node until the optimal value is determined. Excessive depth can lead to Overfitting, leading to poor predictive performance, so proper control is required. Based on Figure 14b, we confirmed that the error rate was minimal at 0.99% when the maximal depth was 7. When the maximum depth is 7, the Decision tree may generate an optimal prediction value. The optimal predicted value was derived when the depth of the Decision tree was 6, and Figure 14 shows how the Decision Tree makes decisions when the depth was 6. The optimal prediction value was derived when the melt temperature was 285°C or lower; the holding pressure was 63 MPa or higher; the holding time was 2.05 s or higher, and the Ram speed was 17.5 s or less. We assumed that the cooling time was not included among them because the weight of the cooling time was the lowest.

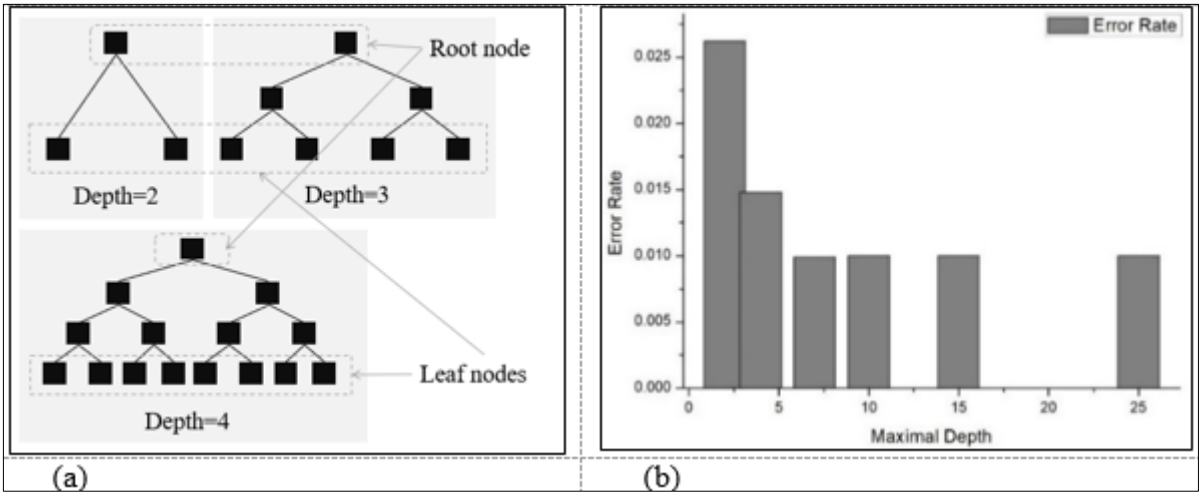

Figure 14. a) Depth of the Decision tree b) error rate according to the maximal depth

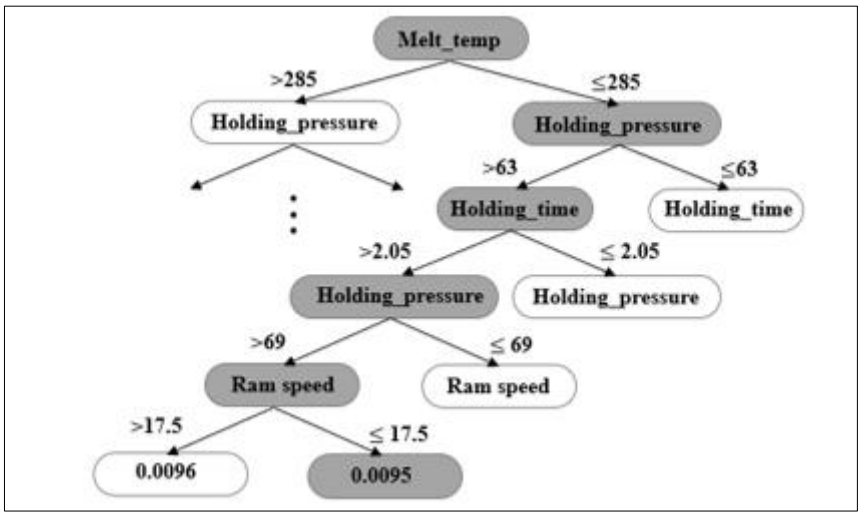

Figure 15. Predicted value when the depth is at 6th

3.4. Discussion

As a result of learning the molding conditions based on the range recommended by Moldflow, the optimal molding conditions predicted by the Decision tree were a melting temperature of 283°C, a cooling time of 16 s, a holding time of 3.7 s, a holding pressure of 70 MPa, and a ram speed of 14 mm/s, and the D_{avg} was 0.0095 mm. Referring to Figure 14, the decision tree shows the path through which we obtained the predicted value.

We created a criterion for evaluating the decision tree's performance if the decision tree's prediction is valid. We conducted one additional molding analysis based on the molding conditions recommended by the Samyang Company, a PC Trirex 3022IR supplier. This criterion will be an indicator to confirm whether the decision tree prediction has contributed to reducing deformation. D_{avg} was confirmed to be 0.0106 mm and was set based on this value, and Table 6 shows the results in detail. Therefore, we demonstrated that the molding condition predicted by the Decision tree improved the deformation by about 10.37% compared to the criterion. Therefore, it is thought that reducing this deformation will help diffuse light uniformly because the part where we measured the deformation is the part where light diffuses among the parts.

In addition, to verify the Decision tree's accuracy, we performed molding analysis under the same conditions as the molding conditions predicted by the Decision tree. As a result, it was confirmed that the error range was 0.0003 mm, and the error percentage was 3.16%. Table 7 shows the accuracy between the D_{avg} predicted by the Decision tree and the D_{avg} derived by the molding analysis.

Table 6. Analysis result of the Decision tree, CAE and criterion

Parameters	A	B	C	D	E	Predicted D_{avg}
Decision tree	283	16	3.7	70	14	0.0095
CAE result	283	16	3.7	70	14	0.0098
Criterion	285	16	4	47.5	15	0.0106

Table 7. Comparison between the Decision tree results and Analysis results

	Prediction	CAE result	Error	% Error
Values	0.0095	0.0098	0.0003	3.1579

Table 8 shows the molding analysis results under the molding conditions predicted by the Decision tree and the molding analysis results under the molding conditions as a criterion. Figure 16a represents the fill time result value; b represents the maximum injection pressure; c represents the maximum clamping force, and d represents the mold temperature result value.

Table 8. Analysis result of the CAE and criterion

	Fill time	Max. injection pressure	Max. clamp force	Mold temp.
CAE result	0.8026	77.24	14.19	47.30~84.37
Criterion	0.7556	83.26	9.44	47.38~84.57

	CAE result	Criterion
(a)	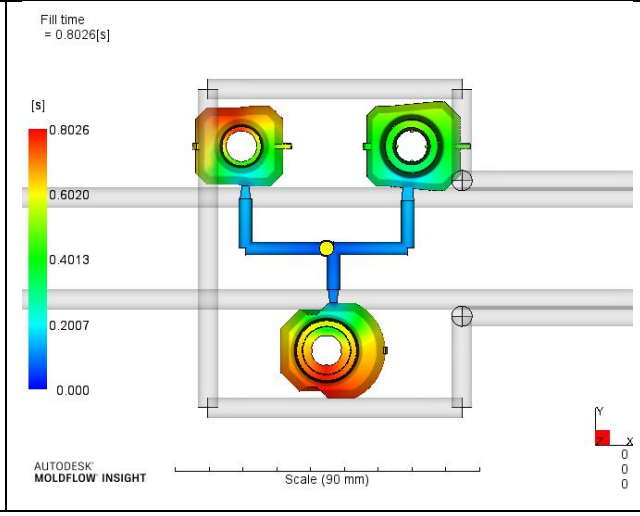	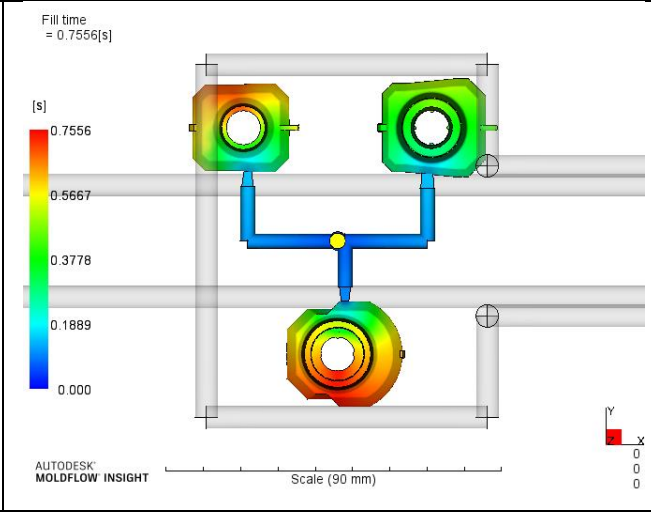

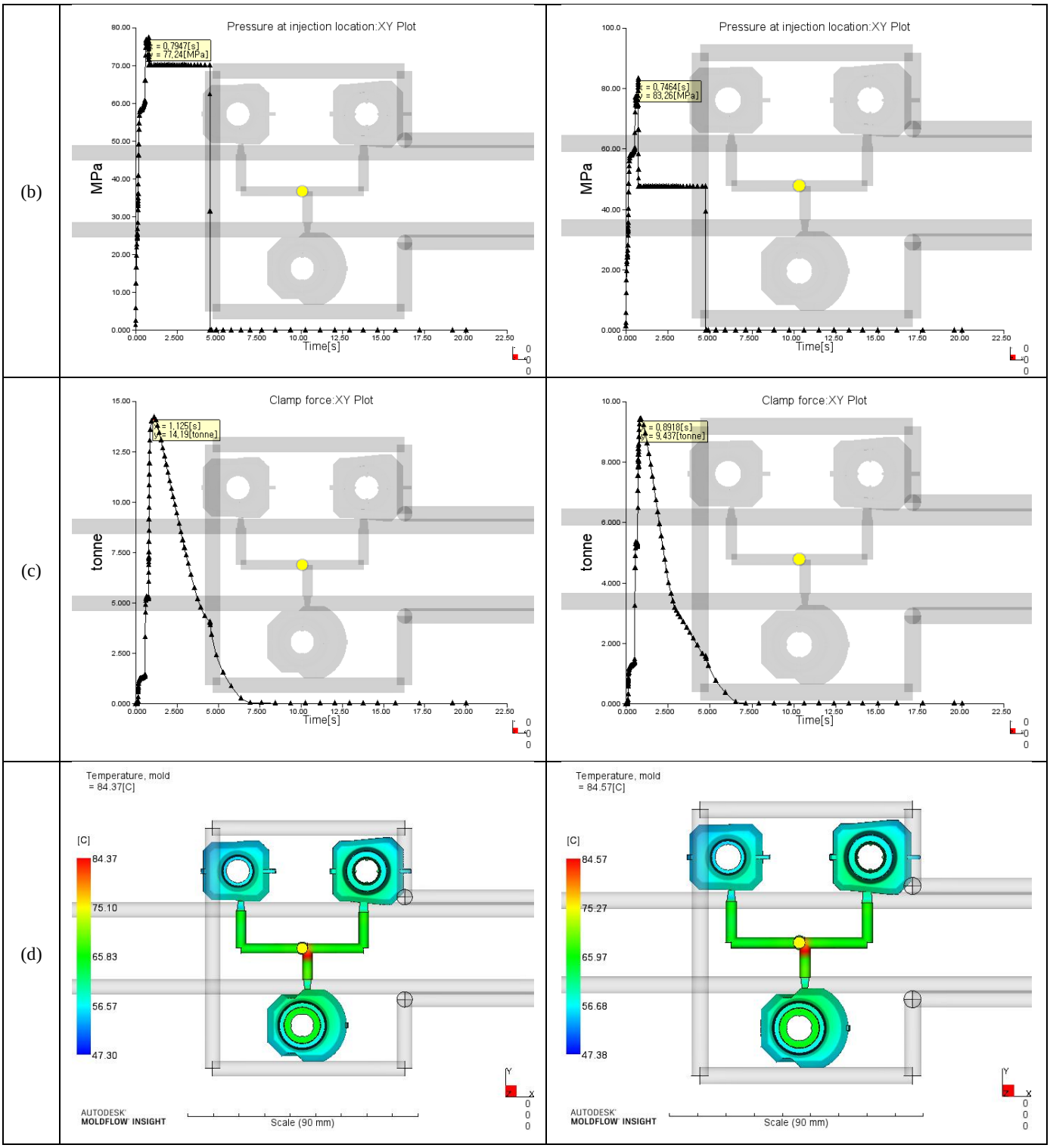

Figure 16. Results of the analysis based on the predicted optimal parameters: a) fill time b) pressure at injection location c) clamp force d) mold temperature

4. Conclusions

This paper applied the Decision tree model to optimize the concentricity deformation of the Lensknob, a small light-guide injection. We conducted 243 injection molding analyses, and as a result, training data were generated. Additionally, we trained the Decision tree with the training data. We designated the axial concentricity after deformation as the target, and the optimal process parameters for minimizing the target were derived using the Decision tree. As a result of the Decision

tree analysis, we confirmed that the variable that had the most significant influence on decision-making was the melt temperature. The variable that had the slightest effect was the cooling time. In addition, we confirmed that the predictive performance of the Decision tree was the best when the maximum depth of the tree was 7, and the minimum of the target was when the depth was 6th. Finally, the predicted optimal molding parameters are a melting temperature of 283°C, cooling time of 16 s, holding time of 3.7 s, holding pressure of 70 MPa, and ram speed of 14 mm/s.

In conclusion, in this study, the deformation of small light-guide injection products was predicted using the Decision tree model and improved by 10.37% from a value of 0.0106 in the criterion. In addition, to confirm the accuracy of the Decision tree, as a result of performing injection molding analysis and comparing it with the optimal parameters derived using Moldflow, we confirmed the target value (axial concentricity after deformation) to be 0.0098 mm. Therefore, the results of injection molding analysis showed an error rate of 3.16% from 0.0095 mm, the minimum value predicted by the Decision tree.

References

1.LEE, Y., CHO, J., HAN, S., Optimization of injection molding of automotive plastic horn cover part using Taguchi method and reverse engineering, *Mater. Plast.*, **58**(4), 2021, 114-129
https://doi.org/10.37358/MP.21.4.5537
2.MARTOWIBOWO, S. Y., KASWADI, A., Optimization and simulation of plastic injection process using genetic algorithm and moldflow, *Chinese Journal of Mechanical Engineering*, 30(2), 2017, 398-406, https://doi.org/10.1007/s10033-017-0081-9
3.ZHAO, L., CHEN, B., YANG, M., ZHANG, S., Application of Moldflow software in design of injection mold, *2010 International Conference on Mechanic Automation and Control Engineering*, 2010, 243-245, https://doi.org/10.1109/MACE.2010.5535705
4. IDAYU, N., MD ALI, M. A., KASIM, M. S., ABDUL AZIZ, M. S., RAJA ABDULLAH, R. I., SULAIMAN, M. A., Flow analysis of three plate family injection mold using moldflow software analysis, *In Symposium on Intelligent Manufacturing and Mechatronics*, 2019, 387-398
https://doi.org/10.1007/978-981-13-9539-038
5. YANG, Y., WANG, M., Using Moldflow to optimize the pouring system of bucket injection mold, *In IOP Conference Series: Materials Science and Engineering*, 394(3), 2018, 032065
https://doi.org/10.1088/1757-899X/394/3/032065
6. LU, X., KHIM, L. S., A statistical experimental study of the injection molding of optical lenses, Journal of Materials Processing Technology, 2001, 113(1), 189-195
https://doi.org/10.1016/S0924-0136(01)00606-9
7. LEE, S. W., JOH, H. H., HONG, J. S., LYU, M. Y., Birefringent Analysis of Plastic Lens Injection Molding for Mobile Phone Camera, *Transactions of Materials Processing*, 20(1), 2011, 54-59
https://doi.org/10.5228/KSTP.2011.20.1.54
8.LEE, H. S., JEON, W. T., KIM, S. W., Development of Plastic Lenses for High-Resolution Phone Camera by Injection-Compression Molding. *Transactions of the Korean Society of Mechanical Engineers A. The Korean Society of Mechanical Engineers, 37(1)*, 2013, 39-46
https://doi.org/10.3795/KSME-A.2013.37.1.039
9. SANO, T., IYODA, Y., SHIMAZU, T., HARUMOTO, M., INOUE, A., NAKABAYASHI, M., ITO, H., Injection Molded Optical Lens Using a Heat Resistant Thermoplastic Resin with Electron Beam Cross-Linking, *Japanese Journal of Applied Physics*, 49(5R), 2010, 052601.
https://doi.org/10.1143/JJAP.49.052601
10.YU, J. C., HUANG, M. S., LIANG, Z. F., & GU, H. H., Intelligent optimization of the replication of injection molding light guide plates using rapid mold surface inducting heating, *In 2011 4th International Conference on Intelligent Networks and Intelligent Systems*, 2011, 65-68
https://doi.org/10.1109/ICINIS.2011.24

11.GAO, Y., WANG, X., Surrogate-based process optimization for reducing warpage in injection molding, *Journal of Materials Processing Technology*, 209(3), 2009, 1302-1309 https://doi.org/10.1016/j.jmatprotec.2008.03.048
12.GAO, Y., TURNG, L. S., & WANG, X., Adaptive geometry and process optimization for injection molding using the Kriging surrogate model trained by numerical simulation, *Advances in Polymer Technology*, 27(1), 2008, 1-16, https://doi.org/10.1002/adv.20116
13.GAO, Y., TURNG, L. S., & WANG, X., Process optimization and effects of material properties on numerical prediction of warpage for injection molding, *Advances in Polymer Technology*, 27(4), 2008, 199-216, https://doi.org/10.1002/adv.20138
14. HWANG, S. H., HAN, S. Y., LEE, H. J., A Study on the Improvement of Injection Molding Process Using CAE and Decision-tree, *Journal of the Korea Academia-Industrial*, 22(4), 2021, 580-586 https://doi.org/10.5762/KAIS.2021.22.4.580
15.AHMED, T., SHARMA, P., KARMAKER, C. L., NASIR, S., Warpage prediction of Injection-molded PVC part using ensemble machine learning algorithm, *Materials Today: Proceedings*, 2020 https://doi.org/10.1016/j.matpr.2020.11.463
16. CHEN, W. C., WANG. M. W., CHEN. C.T., & FU. G. L., An integrated parameter optimization system for MISO plastic injection molding, *The International Journal of Advanced Manufacturing Technology*, 44(5-6), 2009, 501-511. https://doi.org/10.1007/s00170-008-1843-4
17.YANG, D. C., LEE, J. H., YOON, K. H., KIM, J. S., A Study on the Prediction of Optimized Injection Molding Condition using Artificial Neural Network (ANN), *Transactions of Materials Processing*, 29(4), 2020, 218-228, https://doi.org/10.5228/KSTP.2020.29.4.218
18. MOAYYEDIAN, M., DINC, A., MAMEDOV, A., Optimization of Injection-Molding Process for Thin-Walled Polypropylene Part Using Artificial Neural Network and Taguchi Techniques, *Polymers*, 13(23), 2021, 4158, https://doi.org/10.3390/polym13234158
19.ALTAN, M., Reducing shrinkage in injection moldings via the Taguchi, ANOVA and neural network methods, *Materials & Design*, 31(1), 2010, 599-604, https://doi.org/10.1016/j.matdes.2009.06.049
20.TERCAN, H., GUAJARDO, A., HEINISCH, J., THIELE, T., HOPMANN, C., & MEISEN, T., Transfer-learning: Bridging the gap between real and simulation data for machine learning in injection molding, *Procedia Cirp*, 72, 2018, 185-190. https://doi.org/10.1016/j.procir.2018.03.087
21.KE, K. C., HUANG, M. S., Quality prediction for injection molding by using a multilayer perceptron neural network, *Polymers*, 12, 2020, 1812, https://doi.org/10.3390/polym12081812
22. LEE, J. H., PARK, D. Y., JEONG, M. S., HWANG, S. K., CHA, K. J., A Study on Optimization of Injection Parameters by Deep Learning Prediction of Micro Injection Molding, *The Korean Society of Manufacturing Process Engineers*, 29(4), 2021, 238-238, https://doi.org/10.5228/KSTP.2020.29.4.218
23.SHI, H., GAO, Y., WANG, X., Optimization of injection molding process parameters using integrated artificial neural network model and expected improvement function method, *The International Journal of Advanced Manufacturing Technology*, 48(9-12), 2010, 955-962 https://doi.org/10.1007/s00170-009-2346-7
24. OZCELIK, B., ERZURUMLU, T., Comparison of the warpage optimization in the plastic injection molding using ANOVA, neural network model and genetic algorithm, *Journal of Materials Processing Technology*, 171(3), 2006, 437-445, https://doi.org/10.1016/j.jmatprotec.2005.04.120
25.KURTARAN, H., OZCELIK, B., ERZURUMLU, T., Warpage optimization of a bus ceiling lamp base using neural network model and genetic algorithm, *Journal of Materials Processing Technology*, 169(2), 2005, 314-319, https://doi.org/10.1016/j.jmatprotec.2005.03.013
26.TSAI, K. M., LUO, H. J., An inverse model for injection molding of optical lens using artificial neural network coupled with genetic algorithm, *Journal of Intelligent Manufacturing*, 28(2), 2017, 473-487, https://doi.org/10.1007/s10845-014-0999-z
27.SHEN, C., WANG, L., LI, Q., Optimization of injection molding process parameters using combination of artificial neural network and genetic algorithm method, *Journal of materials processing technology*, 183(2-3), 2007, 412-418, https://doi.org/10.1016/j.jmatprotec.2006.10.036

28. XU, Y., ZHANG, Q., ZHANG, W., Optimization of injection molding process parameters to improve the mechanical performance of polymer product against impact, *The International Journal of Advanced Manufacturing Technology*, 76, 2015, 2199–2208
https://doi.org/10.1007/s00170-014-6434-y
29.SON, J. E., KIM, S. B., Rule Selection Method in Decision Tree Models, J*ournal of the Korean Institute of Industrial Engineers*, 40(4), 2014, 375-381, https://doi.org/10.7232/JKIIE.2014.40.4.375
30.***RapidMiner Documentation. (n.d.). Weight by Tree Importance. In rapidminer.com/9.10 Retrieved Dec 23, 2021.
https://docs.rapidminer.com/latest/studio/operators/modeling/feature_weights/weight_by_forest.html

Manuscript received: 18.04. 2022